Int. J. Heat Mass Transfer. Vol. 34, No. 6, pp. 1568–1571, 1991
Printed in Great Britain

0017-9310/91 $3.00+0.00
© 1991 Pergamon Press plc

Mixed convection heat transfer in inclined backward-facing step flows

J. T. LIN, B. F. ARMALY and T. S. CHEN
Department of Mechanical and Aerospace Engineering, University of Missouri–Rolla, Rolla, MO 65401, U.S.A.

(Received 15 March 1990 and in final form 3 July 1990)

INTRODUCTION

IN THIS note mixed convection heat transfer results for two-dimensional laminar flow in an inclined duct with a backward-facing step are presented. The results focus on the effects of inclination angle (buoyancy force) on the flow and heat transfer characteristics under buoyancy-assisting flow conditions. Results on laminar forced convection flow over a backward-facing step have been reported [1–10]. The previous studies, however, did not account for the buoyancy effects on the flow and heat transfer. Recently it has been shown that the buoyancy forces influence significantly the flow and heat transfer characteristics in a vertical duct with a backward-facing step [11]. The present note reports an extension of that study and examines the effects of inclination angle on the flow and heat transfer characteristics under buoyancy-assisting flow conditions.

ANALYSIS

The geometry and the boundary conditions that are used in this study are identical to those used in ref. [11] with the exception that the duct now is inclined as shown in Fig. 1. Under the constant property assumption and the Boussinesq approximation, the governing conservation equations can be written in the non-dimensional form as

$$\frac{\partial U}{\partial X}+\frac{\partial V}{\partial Y}=0 \quad (1)$$

$$U\frac{\partial U}{\partial X}+V\frac{\partial U}{\partial Y}=-\frac{\partial P}{\partial X}+\frac{1}{Re_s}\left(\frac{\partial^2 U}{\partial X^2}+\frac{\partial^2 U}{\partial Y^2}\right)+\frac{Gr_x}{Re_s^2}\theta \quad (2)$$

$$U\frac{\partial V}{\partial X}+V\frac{\partial V}{\partial Y}=-\frac{\partial P}{\partial Y}+\frac{1}{Re_s}\left(\frac{\partial^2 V}{\partial X^2}+\frac{\partial^2 V}{\partial Y^2}\right)+\frac{Gr_y}{Re_s^2}\theta \quad (3)$$

$$U\frac{\partial \theta}{\partial X}+V\frac{\partial \theta}{\partial Y}=\frac{1}{Pr\,Re_s}\left(\frac{\partial^2 \theta}{\partial X^2}+\frac{\partial^2 \theta}{\partial Y^2}\right) \quad (4)$$

where U is the dimensionless streamwise velocity component, u/u_o; u the streamwise velocity component; u_o the average inlet velocity; V the dimensionless transverse velocity component, v/u_o; v the transverse velocity component; X the dimensionless streamwise coordinate, x/s; s the step height; x the streamwise coordinate as measured from the step; Y the dimensionless transverse coordinate, y/s; y the transverse coordinate; P the dimensionless pressure, $(p+\rho gx\cos\gamma+\rho gy\sin\gamma)/(\rho u_o^2)$; p the pressure; γ the angle of inclination from the vertical; ρ the density; g the gravitational acceleration; θ the dimensionless temperature, $(T-T_o)/(T_w-T_o)$; T the temperature; T_o the inlet temperature; T_w the temperature of the heated wall; Re_s the Reynolds number, $u_o s/v$; $Gr_x=Gr_s\cos\gamma$; $Gr_y=Gr_s\sin\gamma$; Pr the Prandtl number, v/α; Gr_s the Grashof number, $g\beta(T_w-T_o)s^3/v^2$; α the thermal diffusivity; β the volumetric thermal expansion coefficient; and v the kinematic viscosity. The thermal properties are evaluated at the film temperature $T_f=(T_o+T_w)/2$.

The boundary conditions are given below.

(a) Upstream inlet conditions at $X=-X_i$ and $1\leqslant Y\leqslant H/s$:

$$U=u_i/u_o,\quad V=\theta=0 \quad (5a)$$

$$u_i/u_o=6[-y^2+(H+s)y-Hs]/(H-s)^2 \quad (5b)$$

where H is the channel height at the exit; h the channel height at the inlet; u_i the local inlet velocity; x_i the inlet length upstream of the step; and $X_i=x_i/s$.

(b) Downstream exit conditions at $X=X_e$ and $0\leqslant Y\leqslant H/s$:

$$\partial U/\partial X=\partial^2\theta/\partial X^2=\partial V/\partial X=0 \quad (5c)$$

along with an overall mass conservation check at the exit, and where x_e is the calculation domain downstream of the step; and $X_e=X_e/s$.

(c) Straight wall at $Y=H/s$ and $-X_i\leqslant X\leqslant X_e$:

$$U=V=\theta=0. \quad (5d)$$

(d) Stepped wall:

upstream of the step, at $Y=1$ and $-X_i\leqslant X\leqslant 0$

$$U=V=\partial\theta/\partial Y=0; \quad (5e)$$

at the step at $X=0$ and $0\leqslant Y\leqslant 1$

$$U=0,\quad V=0,\quad \partial\theta/\partial X=0; \quad (5f)$$

downstream of the step at $Y=0$ and $0<X\leqslant X_e$

$$U=V=0,\quad \theta=1. \quad (5g)$$

The length x_e from the step to the downstream end of the calculation domain was chosen to be 100 steps (i.e. $X_e=100$). Calculations have verified that the flow will become fully developed at the end of this section. The length x_i for the upstream calculations domain was chosen to be five steps (i.e. $X_i=5$). Details of the solution scheme are given in ref. [11].

The results presented in this study were generated by using a non-uniform grid density of 128×50. The number of grid points used in the x-coordinate for the upstream inlet domain (which is five steps) were limited to 15 grid points. The remaining 113 grid points in the x-coordinate were distributed along the calculation domain downstream of the step (which is 100 steps long). The computer program was run on a CRAY X/MP supercomputer, and a solution converged in less than 1000 iterations while utilizing approximately 2–4 min of CPU time.

RESULTS AND DISCUSSIONS

In this study attention is focused on a specific backward-facing step geometry, with an expansion ratio of 2 and a step height of 0.48 cm. The straight wall of the duct is maintained at the inlet air temperature of 20°C. The stepped wall of the duct is maintained adiabatic for the upstream section of the step and for the step itself, while the downstream section behind the step is maintained at a higher but uniform temperature of 35°C. It has been assumed in this study that the flow remains stable and laminar throughout the calculation

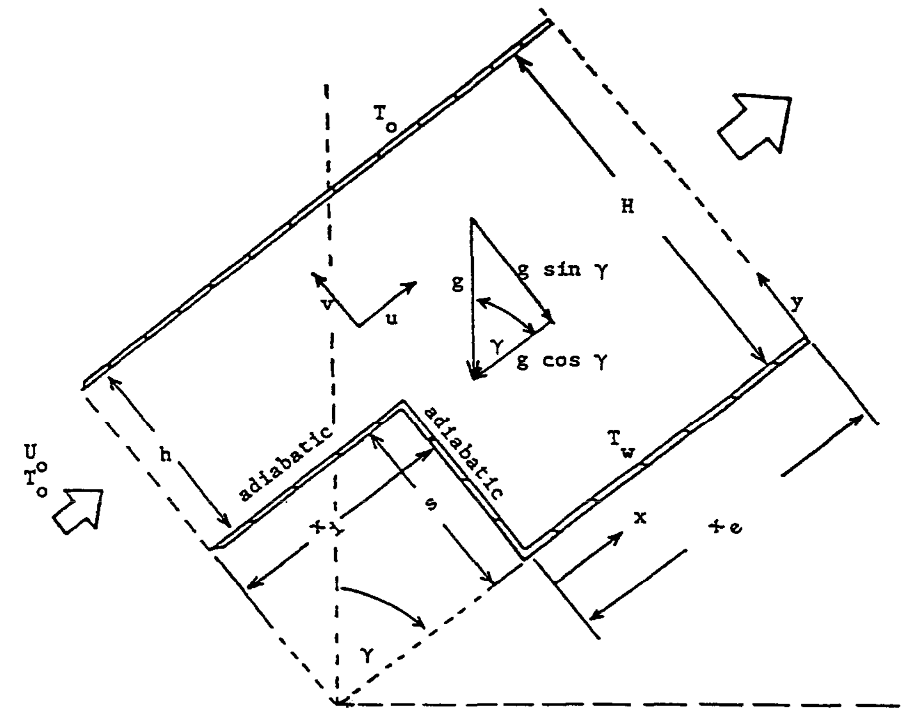

FIG. 1. Schematic of flow domain.

domain, an assumption which must be verified experimentally. The inclination angle was varied while the other variables were fixed to study its effect on the flow and heat transfer characteristics. Calculations were performed for a Reynolds number Re_s of 50.

The developments of the velocity and the temperature profiles throughout the calculation domain are shown, respectively, in Figs. 2 and 3. These two figures display the behaviors of the velocity and the temperature profiles at several downstream locations, for several inclination angles. The development of the velocity distribution from its inlet parabolic distribution to its fully developed distribution far downstream from the step, Fig. 2, indicates that the fully developed velocity distribution is different for different inclination angles (i.e. different values of the streamwise buoyancy parameter) and could include regions of reversed flow, as discussed by Aung and Worku [8]. Approximate analytical expressions for the fully developed velocity and temperature distributions were developed by neglecting Gr_y in the Y-momentum equation and are given by

$$U = Gr_x/Re_s\,(-\tfrac{1}{12}Y^2+\tfrac{1}{4}Y-\tfrac{1}{6})Y-\tfrac{3}{4}Y^2+\tfrac{3}{2}Y \tag{6}$$

$$\theta = \tfrac{1}{2}Y. \tag{7}$$

The transverse component of the Grashof number, Gr_y, has a small effect on the velocity and temperature profiles in the fully developed regime, and a good agreement (less than 1% error) exists between the numerically predicted and the analytically derived fully developed profiles. The analytical treatment neglected the effects of Gr_y but that parameter was a part of the numerical solution. The streamwise component of the Grashof number, Gr_x, is the parameter that strongly influences the flow behavior.

As the angle of inclination increases, the streamwise buoyancy force decreases and the reattachment length increases. Similarly, the temperature profiles, Fig. 3, develop through the separation region from its inlet uniform distribution to its fully developed linear distribution far downstream from the step. The fluid temperature increases as the inclination angle increases, as can be seen in Fig. 3. This latter behavior is attributed directly to the changes in the velocity distribution and the required energy balance.

The Nusselt number at the heated and the unheated wall as defined by $Nu_s = [(T_w-T_0)/(T_w-T_b)](-\partial\theta/\partial Y)|_{Y=0}$ for the heated wall and $Nu_s = [(T_w-T_0)/(T_b-T_0)](-\partial\theta/\partial Y)|_{Y=H/s}$ for the unheated wall where T_b is the bulk temperature, decreases as the inclination angle from the vertical increases. The effect of inclination angle on the Nusselt number at the heated wall is illustrated in Fig. 4. At the heated wall, the Nusselt number starts with a minimum at the base of the step, increases as a function of distance X from the step to a maximum value at X_n (where $X_n = x_n/s$ and x_n is the location of peak Nusselt number), then decreases asymptotically to its constant fully developed value. At the unheated wall, the Nusselt number increases monotonically as a function of the distance from the step. The fully developed value of the Nusselt number for a given inclination angle is the same at both the heated and unheated walls because a linear temperature profile develops in that region. The effect of inclination angle on the shear stress or the friction factor, $C_f\ Re_s$ (where $C_f = \tau_w/(\rho u_0^2/2)$ and $\tau_w = \mu\partial u/\partial y|_w$), on the heated wall is illustrated in Fig. 5. The shear stress at the heated wall decreases, whereas at the unheated wall it increases, as the inclination angle increases. Results for the unheated wall are not presented graphically due to space limitations. It is also clear from Fig. 5 that the reattachment length, X_r ($X_r = x_r/s$ where x_r is the reattachment length), and the recirculation region behind the step increases as the inclination angle increases. For the conditions presented, reverse flow was not detected adjacent to the unheated wall.

An increase in the inclination angle will result in an increase in the reattachment length as shown in Fig. 6. This increase is due to a decrease in the streamwise buoyancy force caused by the increase in the inclination angle. A higher streamwise buoyancy force induces a higher positive velocity

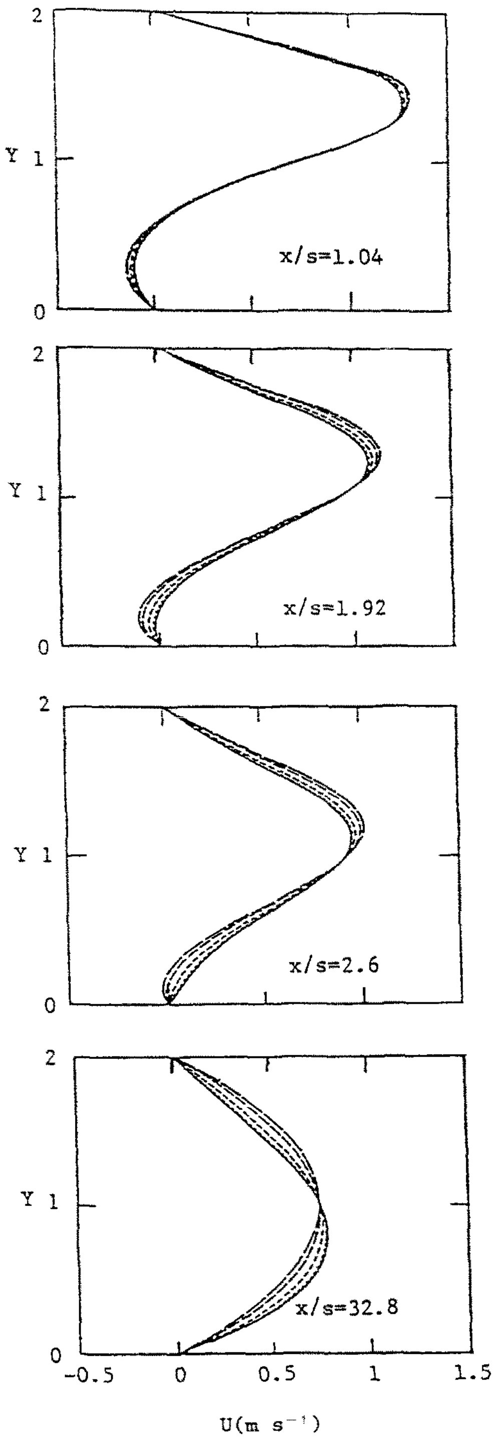

FIG. 2. Effects of inclination angle on velocity distributions ($Re_s = 50$ and $\Delta T = 15$ C) (, $\gamma = 0$; ···, $\gamma = 25$; ---, $\gamma = 50$; , $\gamma = 75$; , $\gamma = 90$).

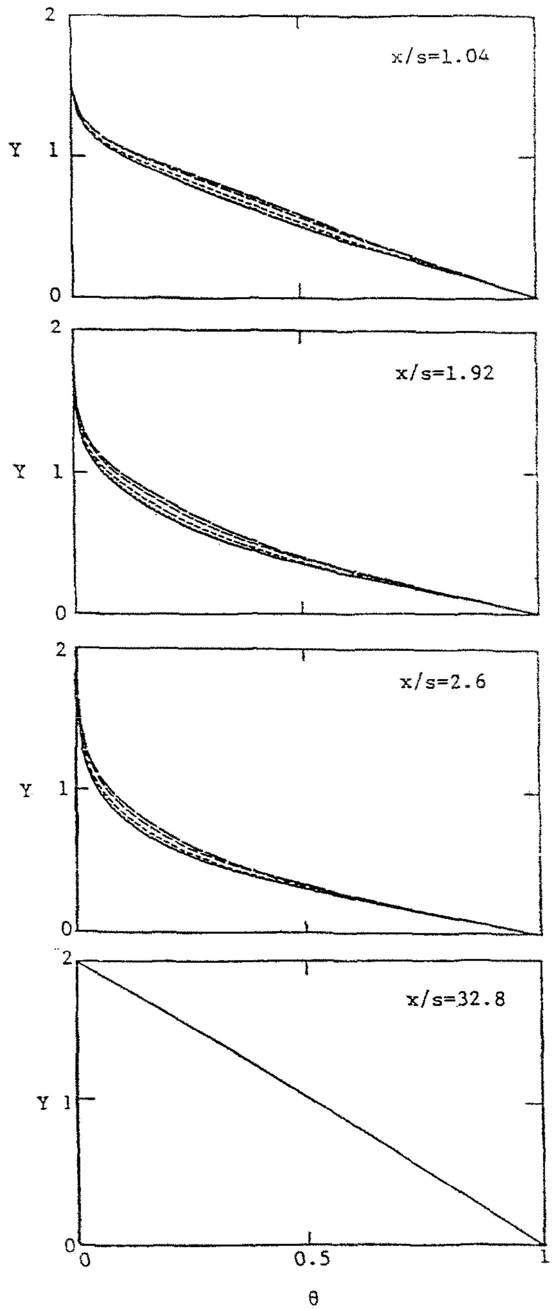

FIG. 3. Effects of inclination angle on temperature distributions ($Re_s = 50$ and $\Delta T = 15$ C) (, $\gamma = 0$; ···, $\gamma = 25$; ---, $\gamma = 50$; , $\gamma = 75$; , $\gamma = 90$).

component near the wall. This will decrease, or cancel, the negative velocity component in the recirculation region, causing the reattachment length to decrease. The location where the Nusselt number at the heated wall reaches its peak value, x_u, also increases, almost linearly, as the inclination angle increases (see Fig. 6).

The results presented indicate that for some convective flow conditions in a backward-facing step geometry, buoyancy effects and/or inclination angle can play a significant role and should be included in the analysis.

Acknowledgement—The study was supported in part by the National Science Foundation under grants CTS-8923010 and CBT-8704896, and by a grant (CBT 88001) from the National Center for Supercomputing Applications at the University of Illinois Urbana/Champaign.

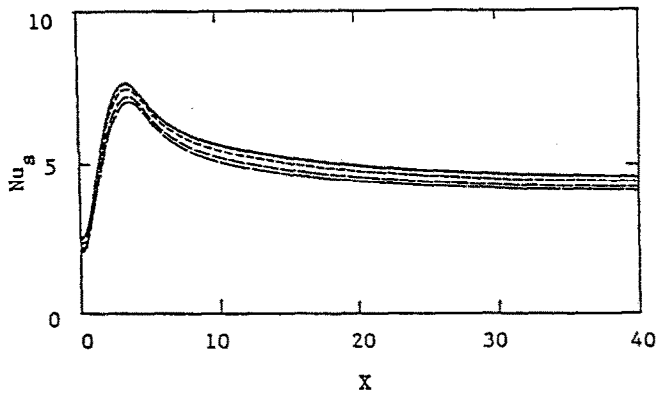

FIG. 4. Effects of inclination angle on the Nusselt number at the heated wall ($Re_s = 50$ and $\Delta T = 15°C$) (——, $\gamma = 0$; · · ·, $\gamma = 25$; - - -, $\gamma = 50$; —-—, $\gamma = 75$; ———, $\gamma = 90$).

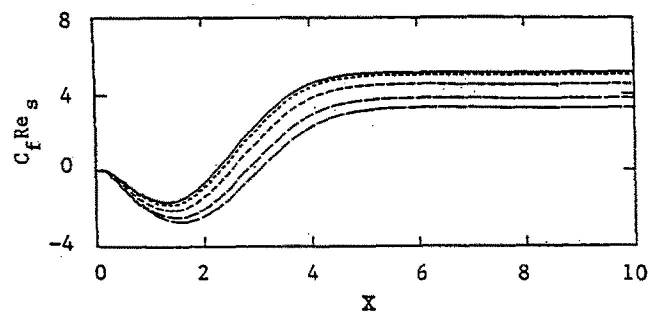

FIG. 5. Effects of inclination angle on the shear stress at the heated wall ($Re_s = 50$ and $\Delta T = 15°C$) (——, $\gamma = 0$; · · ·, $\gamma = 25$; - - -, $\gamma = 50$; —-—, $\gamma = 75$; ———, $\gamma = 90$).

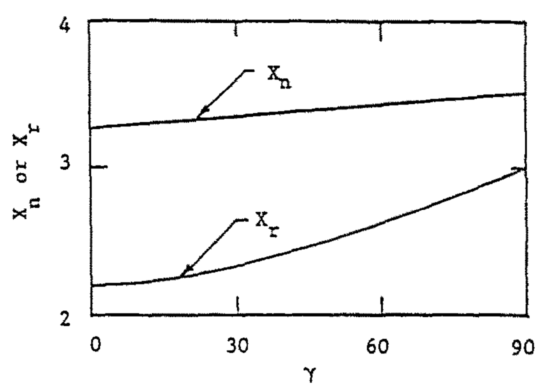

FIG. 6. Effects of inclination angle on reattachment length and the location of maximum Nusselt number ($Re_s = 50$ and $\Delta T = 15°C$).

REFERENCES

1. B. F. Armaly and F. Durst, Reattachment length and recirculation regions downstream of two dimensional single backward facing step. In *Momentum and Heat Transfer Process in Recirculating Flows*, ASME HTD Vol. 13, pp. 1–7 (1980).
2. J. K. Eaton and J. P. Johnson, A review of research on subsonic turbulent flow reattachment, *AIAA J.* **19,** 1093–1100 (1981).
3. R. L. Simpson, A review of some phenomena in turbulent flow separation, *J. Fluid Engng* **103,** 520–530 (1981).
4. B. F. Armaly, F. Durst, J. C. F. Pereira and B. Schounung, Experimental and theoretical investigation of backward-facing step flow, *J. Fluid Mech.* **127,** 473–496 (1983).
5. W. Aung, An experimental study of laminar heat transfer downstream of backsteps, *J. Heat Transfer* **105,** 823–829 (1983).
6. W. Aung, Separated forced convection, *Proc. ASME/JSME Thermal Engng Joint Conf.*, Vol. 2, pp. 499–515 (1983).
7. W. Aung, A. Baron and F. K. Tsou, Wall independence and effect of initial shear-layer thickness in separated flow and heat transfer, *Int. J. Heat Mass Transfer* **28,** 1757–1771 (1985).
8. W. Aung and G. Worku, Theory of fully developed, combined convection including flow reversal, *J. Heat Transfer* **108,** 485–488 (1986).
9. E. M. Sparrow, G. M. Chrysler and L. F. Azevedo, Observed flow reversals and measured–predicted Nusselt numbers for natural convection in a one-sided heated vertical channel, *J. Heat Transfer* **106,** 325–332 (1986).
10. E. M. Sparrow and W. Chuck, PC solutions for heat transfer and fluid flow downstream of an abrupt, asymmetric enlargement in a channel, *Numer. Heat Transfer* **12,** 19–40 (1987).
11. J. T. Lin, B. F. Armaly and T. S. Chen, Heat transfer in buoyancy-assisted, vertical backward-facing step flow, *Int. J. Heat Mass Transfer* **33,** 2121–2132 (1990).